Solar electron source and thermionic solar cell

Parham Yaghoobi, Mehran Vahdani Moghaddam, and Alireza Nojeh

Citation: AIP Advances **2**, 042139 (2012); doi: 10.1063/1.4766942
View online: http://dx.doi.org/10.1063/1.4766942
View Table of Contents: http://aipadvances.aip.org/resource/1/AAIDBI/v2/i4
Published by the American Institute of Physics.

Solar electron source and thermionic solar cell

Parham Yaghoobi, Mehran Vahdani Moghaddam, and Alireza Nojeh[a]
Department of Electrical and Computer Engineering, The University of British Columbia, Vancouver, British Columbia, V6T 1Z4, Canada

(Received 14 August 2012; accepted 24 October 2012; published online 5 November 2012)

Common solar technologies are either photovoltaic/thermophotovoltaic, or use indirect methods of electricity generation such as boiling water for a steam turbine. Thermionic energy conversion based on the emission of electrons from a hot cathode into vacuum and their collection by an anode is also a promising route. However, thermionic solar conversion is extremely challenging as the sunlight intensity is too low for heating a conventional cathode to thermionic emission temperatures in a practical manner. Therefore, compared to other technologies, little has been done in this area, and the devices have been mainly limited to large experimental apparatus investigated for space power applications. Based on a recently observed "Heat Trap" effect in carbon nanotube arrays, allowing their efficient heating with low-power light, we report the first compact thermionic solar cell. Even using a simple off-the-shelf focusing lens, the device delivered over 1 V across a load. The device also shows intrinsic storage capacity. [http://dx.doi.org/10.1063/1.4766942]

Photovoltaics and thermophotovoltaics constitute some of the common methods of solar electricity generation.[1,2] On the other hand, thermionic conversion of heat to electricity has been of interest for a century.[3–5] The fact that the thermionic emission current depends on the cathode temperature exponentially allows one to increase the device efficiency significantly using a small increase in cathode temperature. Naturally, it is highly desirable to have a solar thermionic electricity generator - a device where the cathode is heated using sunlight. Such a device has several potential advantages over its photovoltaic counterpart. In a photovoltaic device, electronic transitions across a band gap (or multiple transitions in more complex structures) are used, and many of the incident photons either lack sufficient energy to contribute to the current, or have excessive energy and heat the device, which is generally detrimental. In contrast, heating is the desired effect in a thermionic device, and can be contributed to by almost all the incident photons. In addition, a thermionic converter is an inherently simple structure and could be less expensive and more robust. In its basic form, it consists of a metal cathode and anode in a vacuum environment, and a lens or mirror to focus sunlight onto the cathode.

In practice, however, the situation is significantly more challenging. This is primarily due to two issues with one common root. When a spot on the surface of a conductor is illuminated by a beam of light, the generated heat spreads to a wide area. This is because good conductors of electricity are normally also good conductors of heat. Consequently, a significant amount of optical energy is required in order for the cathode to reach high temperatures. For example, light-controlled thermionic electron sources used in vacuum-electronic applications, such as accelerators or industrial electron-beam systems, typically use high-power pulsed lasers. Sunlight's average intensity on the surface of the Earth is 0.1 Wcm^{-2}. Focused using a simple lens, this is sufficient to heat a spot on the surface of an insulator to hundreds of degrees - indeed, burning paper with focused sunlight is a favourite childhood pastime. However, a spot on a metallic surface cannot be heated to high temperatures as

[a]anojeh@ece.ubc.ca

easily with this abundant light source, due to the effective dissipation of heat to the surrounding area. Instead, large, expensive and sophisticated light collection and focusing equipment are required.

The second problem also stems from the spreading of the generated heat from the illuminated spot to the surroundings. This creates undesired heating in other parts of the device, which both leads to energy loss/reduced efficiency and can be detrimental to the overall device structure. To mitigate this, thermal isolation of the cathode and/or cooling of the rest of the system are needed, which could add significantly to the complexity, size and cost.

Practical interest in solar thermionic converters goes back over half a century, with many of the efforts focusing on space power applications, such as NASA's Solar Energy Thermionics program,[6] although the technology seems to have been rather dormant for several decades afterward. Around the turn of the century, however, the field has re-emerged with programs such as the High Power Advanced Low Mass (HPALM) solar thermionics system and devices based on the cylindrical inverted converter (CIC) concept. A review of the evolution of solar thermionic devices for space power applications has been presented in Ref. 7. Particularly noteworthy is the fact that all the devices investigated in this context consist of relatively large, complex structures, and require even larger light collection/focusing parts such as mirrors with diameters of a few metres. In addition, typically the cathode is not heated directly; instead, a thermal receiver chamber is used to collect the focused sunlight and generate the required high temperatures. Overall, heating the cathode to thermionic emission temperatures has remained an important challenge (if not the single most important one), to the point that the majority of the tests performed on these devices have involved electric or other means of heating, rather than solar heating. The limited number of on-Sun tests have been conducted in specialized facilities equipped with advanced focusing systems, such as NASA's JPL Table Mountain Facility or the Marshall Space Flight Centre.[7] This highlights the fundamental challenge of heating a cathode using sunlight. Nonetheless, conversion efficiencies as high as 11% have been shown, clearly demonstrating the potential of the technology.[7]

Here, we report a device that overcomes both of the above challenges and lays the foundation for compact thermionic solar cells. Recently, we observed a "Heat Trap" effect in a macroscopic-size array of vertically-aligned carbon nanotubes, known as a carbon nanotube forest. If illuminated by even a low-power laser beam that is focused sufficiently, a spot on the forest sidewall automatically becomes thermally isolated and thus easily heated to thermionic emission temperatures ($>2,000$ K), while retaining electrical conductivity.[8] This "Heat Trap" effect was explained based on the rapid drop of thermal conductivity with temperature in nanotubes, as well as the quasi-one-dimensional nature of heat transport in the forest, in contrast with the situation in an isotropic bulk conductor. This combination leads to a positive feedback mechanism that drives down the thermal conductivity of the irradiated spot, isolating it from the surroundings and allowing its efficient heating.[8] This effect not only allows one to achieve thermionic emission temperatures with a low-power beam of light, but also, given the localized nature of heating, alleviates the issue of heat spread to contacts and other parts of the device. This phenomenon may open the door to applications of thermionic electron sources using readily available light sources. A natural question then arises as to the possibility of solar electricity generation based on this effect.

The light intensity needed to achieve Heat Trap in a nanotube forest depends on the size of the irradiated spot. We have observed that, for a spot with a diameter of a few hundred micrometres, this threshold intensity is on the order of 50 Wcm^{-2}.[8] The Sun's average intensity on the surface of the Earth is 0.1 Wcm^{-2}. Focused 500 times, this seems to be sufficient for our purposes. However, the Heat Trap effect was originally observed using a laser beam. Laser and sunlight have almost no common property: one is monochromatic, the other is not; one is coherent, the other is not; one is stable in time, the other is not. Therefore, it is not clear that a solar device could work, not least since the different wavelengths of the solar spectrum may be absorbed at different rates, plus the fact that a typical lens cannot focus all the wavelengths equally well due to chromatic aberrations. Here, we show that a thermionic solar cell based on this effect is, in fact, possible and quite practical.

The first step is to investigate whether sunlight can heat the nanotube forest sufficiently for thermionic electron emission into vacuum. We built a small portable vacuum chamber from glass (Figure 1(a)). We used a multiwalled carbon nanotube forest, with lateral dimensions of $\sim$5 mm and a height of $\sim$2 mm, grown on a highly-doped silicon wafer (see Appendix A for growth details).

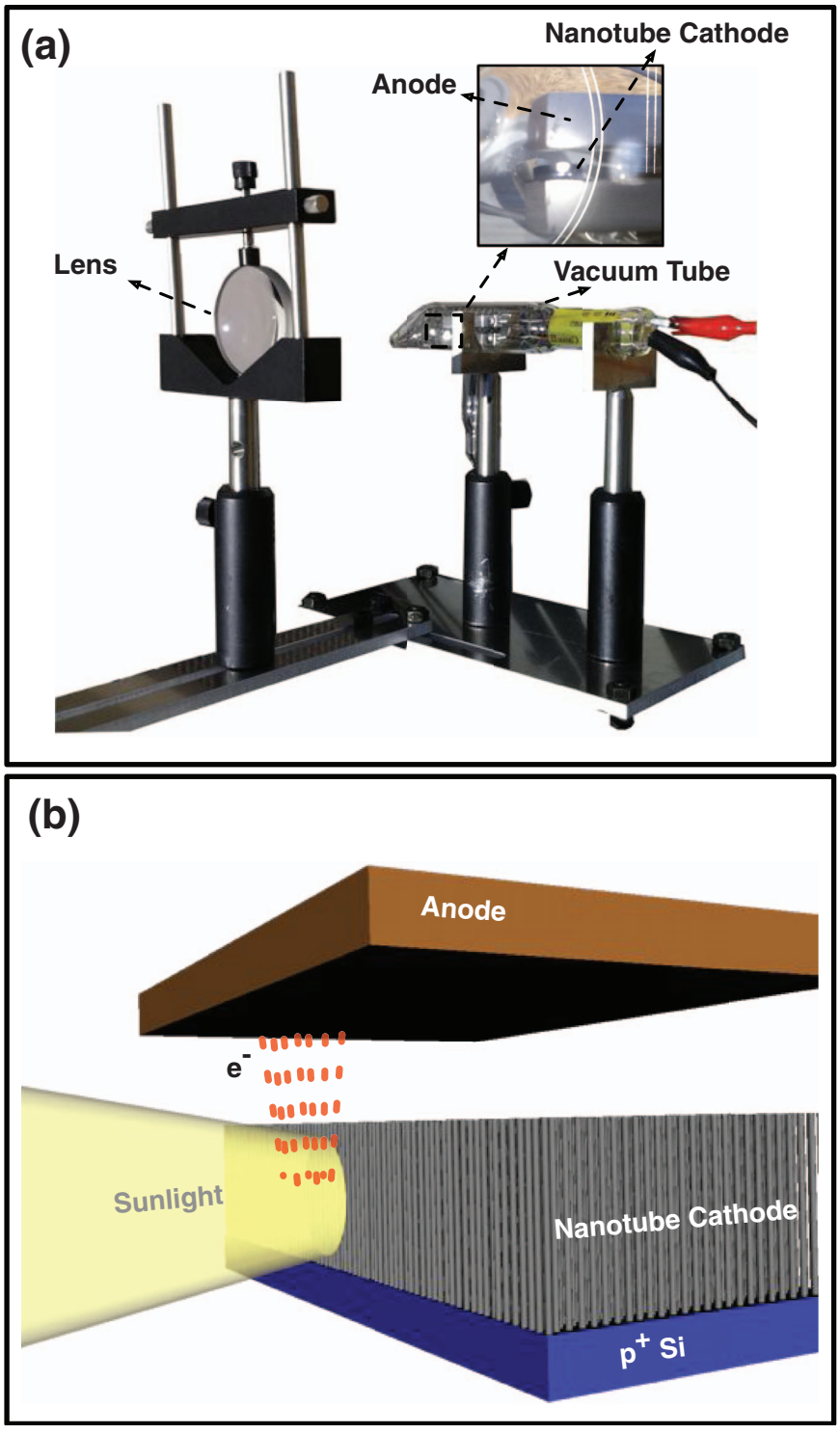

FIG. 1. (a) A solar electron source in a simple glass vacuum tube. The nanotube forest was grown on a highly doped silicon wafer (see Appendix A for detail), which was mounted on a metallic holder and constituted the cathode, and placed below another metallic piece, which served as the anode. The cathode and anode were connected to a Keithley 6517A electrometer through glass-metal electric feedthroughs. The glass tube was pumped down using a dry turbo-molecular pump and sealed at 10^{-9} Torr. The vacuum tube was mounted on a holder where a lens focused sunlight onto the sidewall of the forest. Inset shows a magnified view of the electrodes, the nanotube forest and the focused solar irradiation spot. (b) A schematic representation of the device (not to scale). The focused sunlight induces local heating of the nanotube forest surface to thermionic emission temperatures, and the anode, placed above the forest, collects the emitted electrons.

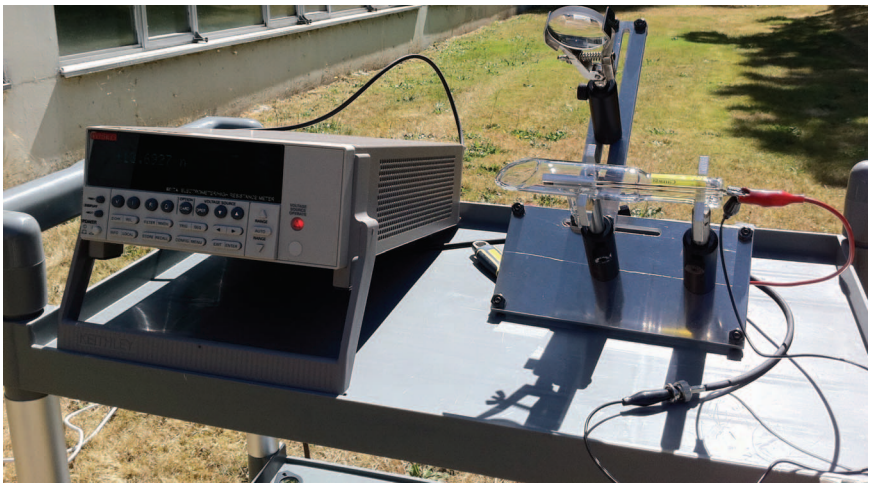

FIG. 2. Experimental setup of the solar electron source in the courtyard behind our laboratory. An off-the-shelf, 50-mm-diametre lens was used to concentrate sunlight onto a ∼700-μm spot on the side surface of the carbon nanotube forest, which was placed inside the glass vacuum tube. To apply a collection voltage and measure the electron emission current, a Keithly 6517A electrometer was used.

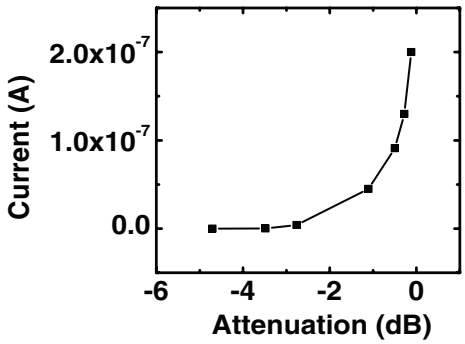

FIG. 3. The thermionic electron emission current of the solar electron source versus the solar power shows a non-linear behaviour, as expected. The illuminated spot was ∼700 μm in diameter in this case. A collection voltage of 50 V was applied, which is significantly below the field-emission threshold, given the cathode-anode distance of ∼1 mm. A broadband, variable, neutral-density filter was used to attenuate the sunlight in order to obtain the various power levels indicated on the horizontal axis.

The forest was placed inside the chamber on a metal electrode. Another electrode (electron collector or anode) was placed ∼1 mm above the top surface of the forest. Electric feedthroughs allowed the application of a collection voltage between the anode and the cathode, as well as the measurement of the sunlight-induced thermionic electron emission current. Figure 1(b) shows a schematic of the device. Using an off-the-shelf glass lens with a diameter of ∼50 mm, sunlight was focused onto a spot with a diameter of ∼700 μm on the sidewall of the nanotube forest. To calculate the intensity, we used the data for solar irradiation for the time of the experiments (moderately sunny days with an average temperature of 22 °C in the months of August and September 2011 in Vancouver, British Columbia, Canada) available from the Natural Resources Canada database.[9] An average mean global insolation of 0.68-0.78 Whcm^{-2} was reported, which translates to an intensity of 0.0283-0.0325 Wcm^{-2}. Therefore, a total of 0.555-0.638 W of power was collected by our 50-mm-diameter lens, which, focused to the 700-μm spot, translates into an intensity of 144-166 Wcm^{-2} (for a focusing ratio of ∼5,100). This is above the Heat Trap threshold of 50 Wcm^{-2}, notwithstanding the differences between laser and sunlight mentioned previously. Figure 2 shows a photo of the experimental setup on a movable cart in the courtyard behind our laboratory. (Note the simplicity of this device compared to the designs reviewed in Ref. 7). We also placed an attenuator in front of the lens in order to investigate the device response to optical power. Figure 3 shows the electron

emission current as a function of solar power when a collection voltage of 50 V was applied to the anode, demonstrating the operation of a thermionic solar electron source.

For a thermionic solar cell, the goal is electricity generation in absence of a collection voltage, or under a reverse collection voltage (operation in the second or fourth quadrants of the current-voltage characteristics). For such operation, one relies on the emitted electrons reaching the anode due to their kinetic energy upon emission from the cathode surface, rather than being assisted by the anode voltage. Therefore, the anode structure and cathode-anode distance become very important for the efficient collection of the emitted electrons. We built a new device, this time using a slightly wider anode placed at ∼1 mm above the nanotube forest surface. (The anode was extended to cover an area in front of the electron-emitting side of the nanotube forest in order to improve the collection of electrons.) Figure 4(a) shows the emission current as a function of applied voltage. The green highlighted area illustrates the power generation regime, where electrons reach the anode despite its negative bias, and the device delivers electric power to the biasing electrometer (Figure 4(b)). As the ultimate operational test, we disconnected the cathode/anode terminals from the biasing electrometer and simply connected them across a 10-MΩ resistor (Figure 4(c)), where we measured a generated voltage of ∼60 mV. Figure 4(d) illustrates the generated current and power density of the solar cell, calculated based on the data of the green section of Figure 4(a) and the electron emission area. (Note that, in keeping with the convention often used in photovoltaics, on this graph we are showing the magnitude of the generated voltage and have dropped the negative sign.) At the peak output power point, given the input optical power mentioned previously, the conversion efficiency can be calculated to be $\sim 10^{-6}\%$.

Arguably, the efficiency of this crude, first prototype is extremely low; however, major improvement should be possible. Engineering the device geometry in terms of cathode and anode structure and relative placement could increase the efficiency significantly; efficiencies of over 30% have been predicted for thermionic converters.[10,11] In the case of solar thermionic devices, 7% has been achieved by some of the NASA devices described previously.[7] Therefore, the low efficiency of our first prototype is clearly not a fundamental limit. Indeed we have increased the efficiency of our device by two orders of magnitude by simply placing an indium-tin-oxide transparent anode close to the sidewall of the nanotube forest (as shown in Figure 5(a)) and focusing the sunlight with an aspherical lens. Illumination now takes place through the transparent anode, and the placement of the anode immediately in front of the electron-emitting spot allows for more efficient collection of the electrons. The aspherical lens enables better solar concentration and thus leads to higher operating temperatures. Figure 5(b) shows the emission current as a function of applied voltage of the improved prototype, which illustrates a larger power generation area as compared to Figure 4(a). As before, for an example operational test we connected a 10-MΩ resistor and measured a generated voltage of ∼1.3 V. An improved peak energy conversion efficiency of $\sim 10^{-4}\%$ can be calculated using the generated power density curve (shown in Figure 5(c)) and the solar irradiance data of April of 2012 in Vancouver, British Columbia, Canada.[9] Although the efficiency of this prototype is still low, note that the simple modifications made to the anode and lens led to an improvement of two orders of magnitude compared to the first device. More importantly, as can be seen on Figure 5(c), this simple device produces a short-circuit current density of 13 mAcm^{-2} and a peak power density of 4.2 mWcm^{-2}, which are already comparable to those of advanced photovoltaic cells.[12] In addition, the open-circuit voltage of ∼3.5 V achieved by this device is significantly higher than that of most photovoltaic devices. The significant increase in efficiency of our second prototype is due primarily to the exponential nature of thermionic emission; a slight improvement in the focusing of sunlight and thus increase in temperature (plus a better placement of the anode) greatly enhanced the performance. Below we discuss some of the issues specific to our device and present a simple model to evaluate efficiency by considering the various energy loss mechanisms.

At constant cathode temperature, conservation of energy dictates that the optical power delivered to the illuminated spot on the cathode be equal to the total power leaving the spot due to three mechanisms: electron emission, black body radiation and heat transfer to the areas surrounding the illuminated spot (see Appendix B for the detailed description of the power equilibrium equation). The first mechanism is desirable and must be favoured in order to increase the electricity generation efficiency, while the other two lead to loss. In an isotropic, bulk cathode, heat flows radially outward

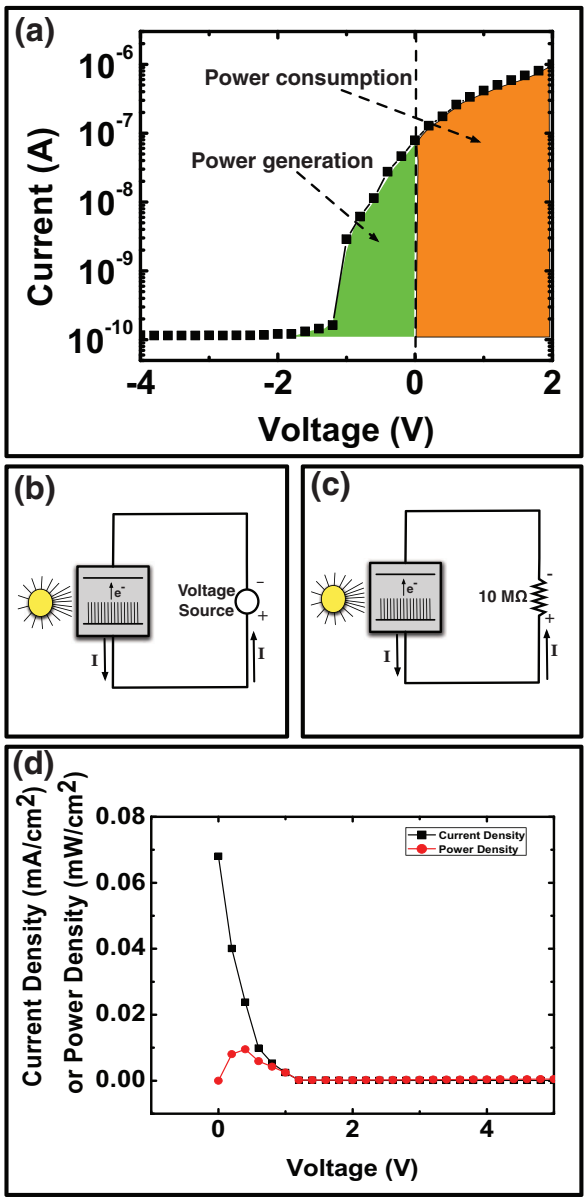

FIG. 4. (a) The thermionic electron emission current of the solar cell versus the applied voltage shows two distinct regions. When the voltage applied to the anode is positive (orange-coloured area), the device acts as a solar electron source where the anode attracts the electrons emitted by the cathode. When the voltage applied to the anode is negative (green-coloured area), the electrons have to surmount the opposing electric field to reach the anode. This region corresponds to electricity generation and energy is delivered by the solar cell to the electrometer (b). When the device is disconnected from the electrometer and simply connected to a resistive load, it creates a voltage across the load and delivers electric power to it (c). (d) The corresponding generated current and power densities of the solar cell (plotted on the positive voltage axis) calculated using a spot diameter of ∼700 μm. Also given the sparse nature of the nanotube forest, only ∼30% of the incident area is covered by nanotubes.

in all directions from the point of generation. This situation is shown in Figure 6(a), where heat flows perpendicularly to the surface of a hemisphere inside the material. On the other hand, the carbon nanotube forest is a highly anisotropic, nanostructured cathode, where the nanotubes are aligned along the growth direction (Figure 1(b)). In such a structure, thermal conductivity along the nanotubes is substantially higher than that in the lateral directions, for instance by a factor of >150 as reported in Ref. 13. For simplicity, we neglect lateral heat conduction. The situation

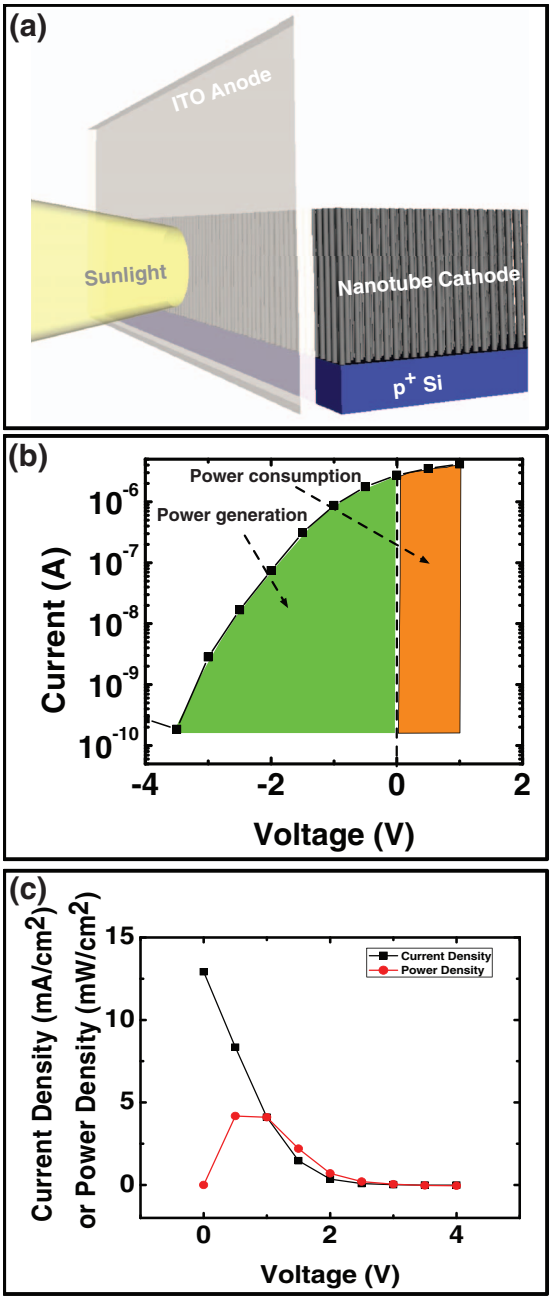

FIG. 5. (a) Schematic of the improved prototype with a transparent indium tin oxide anode (not to scale). (b) Thermionic electron emission current as a function of applied voltage of the improved prototype. (c) The corresponding generated current and power densities of the improved solar cell calculated using a spot diameter of ~300 μm, which is due to better focusing of sunlight with an aspherical lens. Similar to the first prototype, only ~30% of the incident area is covered by nanotubes because of the sparse nature of the nanotube forest.

is shown in Figure 6(b), where heat propagates only upward and downward from the illuminated spot.

Using the power equilibrium equation, we calculated the temperature of the illuminated spot and the conversion efficiency as a function of light intensity for the nanotube forest and an isotropic bulk cathode (see Appendix B for the details of the calculation and the differences in the two cases). Figure 7 shows the temperature vs. light intensity for both cases under identical illumination conditions; the anisotropic nature of heat dissipation in the forest and the fast drop of thermal conductivity

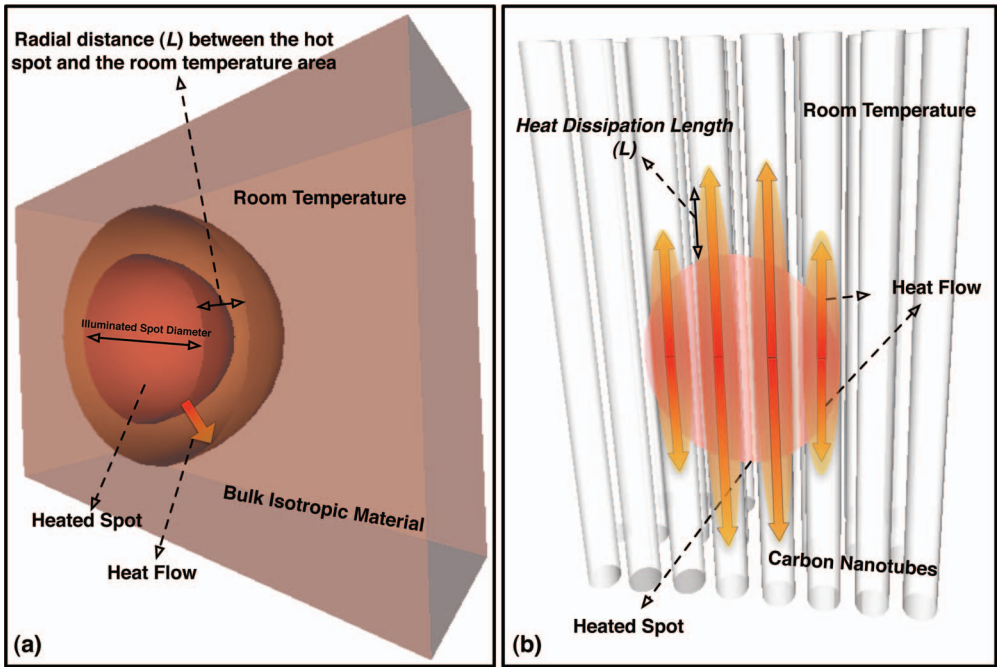

FIG. 6. (a) Schematic of heat flow in an isotropic bulk cathode. Since bulk cathodes are good thermal conductors, heat spreads to an area much larger than the point of generation. The hemispheres indicate the radial flow of heat equally in all directions away from the point of generation. (b) Schematic of heat flow in the carbon nanotube forest. Carbon nanotube forests are highly anisotropic and their thermal conductivity in the axial direction (along the nanotube) is much higher than that in the perpendicular direction (between nanotubes). This practically limits heat propagation to only along the axis of the nanotubes.

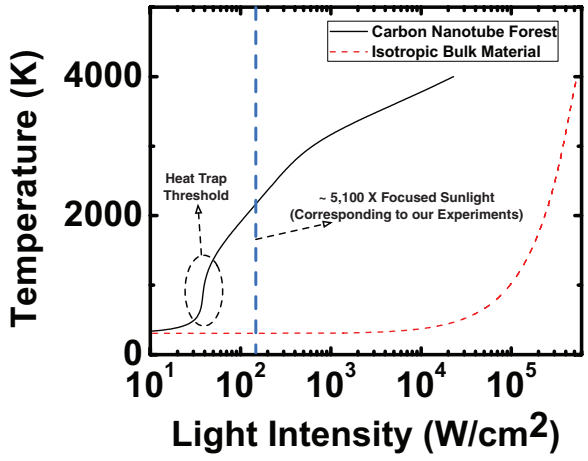

FIG. 7. Temperature as a function of light intensity for an isotropic material with a constant thermal conductivity behaviour and an anisotropic material (i.e. nanotube forest) with a thermal conductivity behaviour of $\frac{1}{\alpha T+\beta T^2}$. The temperature of the carbon nanotube forest increases much more rapidly than that of a bulk material. This is because heat can only flow in one dimension in an anisotropic material as opposed to flowing in all three dimensions. Also, nanotubes exhibit a more rapid drop in thermal conductivity than bulk materials as a function of temperature. The parameters used to obtain these curves were: $\Phi = 4.5$ eV, $T_{room} = 300$ K, and $r = 350$ μm. For an isotropic material such as tungsten, $k(T) = 138$ Wm^{-1}K^{-1},[14] $\epsilon = 0.04$, and $L = 400$ μm; for an anisotropic material such as the carbon nanotube forest, $\alpha = 3.7 \times 10^{-7}$, $\beta = 9.7 \times 10^{-10}$, $\epsilon = 1$, and $L = 42$ μm. By solving the electromagnetic wave equation[15], the penetration depth of light, d, was calculated to be $\sim$50 nm.

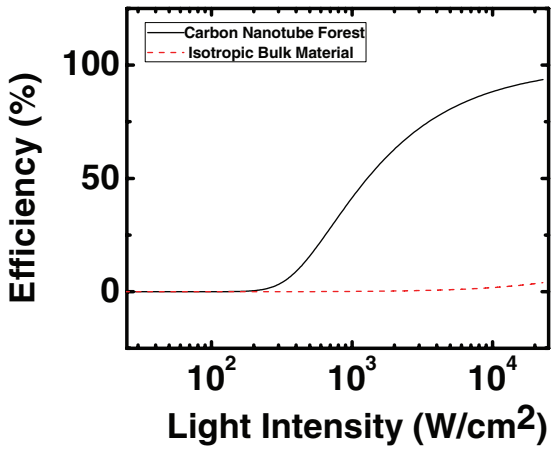

FIG. 8. Efficiency as a function of light intensity for the carbon nanotube forest cathode and a bulk cathode. The efficiency of the carbon nanotube forest is predicted to be much higher than that of the bulk material at practical light intensities. This is because the Heat Trap effect allows the carbon nanotube forest to heat up to higher temperatures with lower light intensities. The parameters used to obtain these curves were the same as those used for Figure 7. Please note that the model used for the carbon nanotube forest cathode and the bulk cathode does not include the space-charge effect. Therefore, efficiencies of 100% are not realistic in either case.

with temperature lead to a much faster increase of temperature at significantly lower light intensity. The Heat Trap threshold is indicated on the figure, beyond which heat transfer to the surroundings is negligible and the illuminated spot is effectively thermally isolated, in sharp contrast with the situation in the bulk material.

The relative contribution of electron emission to the incident solar power gives the electricity conversion efficiency. Figure 8 shows the efficiency for the cases of a regular bulk cathode and a carbon nanotube forest cathode, where it can be seen that the latter strongly outperforms the former. This is due to the Heat Trap effect, resulting in a much higher temperature in the nanotube forest compared to the bulk material and, therefore, a much higher thermionic electron emission current, which is an exponential function of temperature. Under a practical sunlight concentration of $\sim$5, 000 $\times$, obtainable in a simple, compact device like the one reported here, the nanotube forest allows the creation of a thermionic solar cell, whereas a bulk cathode requires $>$1, 000 times higher intensity to achieve the same temperature (see Figure 7), as seen in previous thermionic solar converters such as the NASA experiments mentioned before. Indeed, we tested a piece of copper as cathode and were not able to measure any emission current by focusing sunlight using our simple lens (our measurement setup was capable of detecting currents as low as 10 pA).

The trend shown in Figure 8 is based on a simple model and optimistic. In practice, a significant portion of the energy of the emitted electrons is not converted to useful energy in the external load. Several key issues need to be addressed. Firstly, the device structure must be designed so as to improve the electron collection efficiency of the anode. Space charge effects also pose a limit on the conversion efficiency of thermionic devices: the Coulomb repulsion of the emitted electron cloud near the cathode surface restricts the emission of subsequent electrons. The situation can again be improved by reducing the anode-cathode distance. Once the Heat Trap threshold (see Figure 7) is achieved, the heat transfer rate (third term on the right-hand side of eq. (1) in Appendix B) becomes negligibly small, and black body radiation (the second term) remains the dominant power loss mechanism. Operating at lower temperatures (albeit above the Heat Trap threshold) would reduce this loss, but would also reduce the electron emission current, which is undesirable. However, if the workfunction of the nanotubes could be reduced (or a similar, one-dimensional material with lower workfunction could be used), the electron emission current would increase significantly for a given temperature and, therefore, the device could operate at lower temperature with higher efficiency. This can be seen from Figure 9, which shows the efficiency as a function of temperature for various cathode workfuntions. Another consideration is the behaviour of the electrical conductivity of the

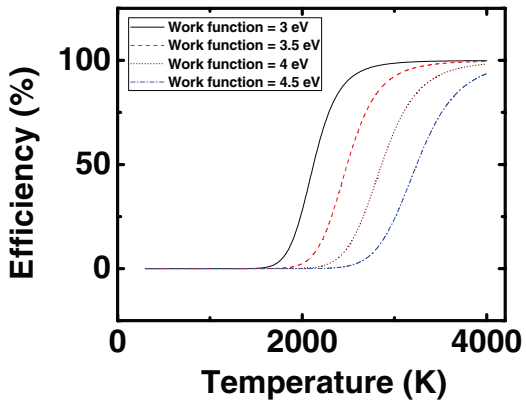

FIG. 9. Efficiency as a function of temperature for anisotropic cathodes with different work functions. Similar efficiencies can be achieved at lower temperatures as the workfunction of the material is reduced. The parameters used to obtain these curves were the same as those used for Figure 7. Similar to Figure 8, the model used for this figure does not include the space-charge effect and, therefore, efficiencies of 100% are not realistic.

illuminated spot at high temperatures. Other practical issues such as using better, achromatic solar concentrators as opposed to our simple glass lens should offer a significant improvement in efficiency.

In summary, as mentioned before, the inherent conversion efficiency of thermionic devices can be over 30%.[10,11] The key contribution of the present report is the demonstration that it is possible to create a compact, simple and inexpensive solar thermionic converter using a nanostructured cathode (in this case a carbon nanotube forest). Further engineering of the device is required in order to raise the efficiency to practical values. Nonetheless, the device has several key merits, some of which represent significant advantages over photovoltaic devices: (1) it uses a very wide range of the solar spectrum, (2) it is capable of generating high current and power densities, (3) its efficiency can be improved significantly by only slightly improving the light focusing mechanism (and thus increasing the cathode temperature), and (4) it has a simple, robust and inexpensive structure. Carbon nanotube forests are good candidates for the cathode as they are excellent light absorbers over a broad spectral range.[16,17] Indeed, we have observed that laser beams of various wavelengths from ultra-violet to infrared can be used for efficient heating of the nanotube forest through the Heat Trap effect (results not shown here). In addition, the device could potentially be engineered to use a combination of the photovoltaic and thermionic effects in a scheme similar to the one proposed by Schwede *et al.*.[18] Another significant advantage of the thermionic solar cell is its inherent storage capacity. Given the vacuum gap between the cathode and anode, once electrons are collected by the anode, there is no return path for them to the cathode, except through an external load. In absence of a load, continuous electron emission by the cathode leads to a gradual voltage increase across the device (charging of the cathode-anode capacitor). Eventually, the anode voltage becomes sufficiently negative to block any further electrons from being collected, and the voltage saturates. In our improved prototype, we measured a built-up voltage of 3.5 V without any load (except for the high-resistance voltmeter circuit). This characteristic of the device is all the more promising given the high surface area of nanotubes, which creates opportunities for engineering solar cells with large inherent capacitance for electricity storage: solar rechargeable batteries.

ACKNOWLEDGMENTS

We acknowledge financial support from the Natural Sciences and Engineering Research Council, the Canada Foundation for Innovation, the British Columbia Knowledge Development Fund, the BCFRST Foundation and the British Columbia Innovation Council. Parham Yaghoobi thanks the Department of Electrical and Computer Engineering and the University of British Columbia for additional support.

APPENDIX A: CARBON NANOTUBE FOREST GROWTH

Arrays of vertically-aligned, millimetre-long multiwalled carbon nanotubes were grown using a chemical vapour deposition reactor on a catalyst layer of 10 nm of alumina and 1-2 nm of iron, which had been evaporated successively on a highly p-doped silicon wafer. The reactor consists of two heating zones; as the gas flows through the system, the first heating zone helps break down the C_2H_4 and H_2 gases and the second heating zone activates the catalyst and enables the growth. By decoupling these processes using two heating zones, one can achieve better control over the growth in terms of forest height.[19] For a typical growth, the first heating zone was heated to 850 °C under 800 sccm of Ar and the second heating zone was heated to about 800 °C under the same flow rate of Ar. The sample was then annealed for 1 min under 800 sccm of Ar and 1,000 sccm of H_2. The growth was initiated by introducing 400 sccm of C_2H_4 and maintaining the flow of Ar and H_2. The nanotube forest reached a height of ∼2 mm after 15 min of growth. Transmission electron microscopy showed the nanotubes to be multi-walled.

APPENDIX B: POWER EQUILIBRIUM AND THE CALCULATION OF CATHODE TEMPERATURE AND EFFICIENCY

The energy conservation (power equilibrium) equation can be written in terms of light intensity as

$$I_{Light} = (\Phi + 2kT)A_G T^2 e^{\frac{-\Phi}{kT}} + \epsilon\sigma T^4 + k(T)\vec{\nabla}T\frac{A_{heat}}{A}, \tag{B1}$$

where A_G is Richardson's constant, T is the temperature of the illuminated spot, k is Boltzmann's constant, Φ is the work function of the material, σ is the Stefan-Boltzmann constant, and ϵ is the emissivity of the material (for which we assume 1 for nanotubes, which are extremely dark materials). $k(T)$ is the temperature-dependent thermal conductivity, and A_{heat} is the cross sectional area of heat flux, to be distinguished from A, the area of the illuminated spot. The first term on the right-hand side of the equation is the power dissipated due to emission of electrons through the thermionic process (the Richardson law) and the second term is the power dissipated through black body radiation (the Stefan-Boltzmann law), both per unit area of the hot (illuminated) spot. The third term describes the loss due to heat transfer to the areas surrounding the hot spot on the cathode.

In the case of an isotropic bulk cathode, the third term in equation (1) takes the form:

$$k(T)\frac{T - T_{room}}{L}\frac{2\pi r^2}{\pi r^2}, \tag{B2}$$

where L is the distance between the hot spot and the room temperature area of the material (see Figure 6(a)) and $k(T)$ can follow a $\frac{1}{\alpha T}$ behaviour[20] or only have a small drop in thermal conductivity over a large range of temperatures. For example, the thermal conductivity of tungsten only drops by ∼25% from room temperature to 2900 K.[14] For simplicity, we have assumed that the hot region consists of a hemisphere with a diameter equal to that of the illuminated spot, with uniform temperature.

In the case of the nanotube forest cathode, the third term in equation (1) takes the form:

$$k(T)\frac{T - T_{room}}{L}\frac{\eta 2rd}{\pi r^2}, \tag{B3}$$

where d is the penetration depth of light in the nanotube forest, r is the radius of the illuminated spot, and η is the percentage of the area that is covered by nanotubes in the plane perpendicular to their axis. This is about 30% in a typical carbon nanotube forest. Here, for simplicity we have assumed that the region with depth d behind the illuminated spot has uniform temperature.

In addition, the behaviour of thermal conductivity as a function of temperature has been reported to be different in nanotubes compared to a bulk solid; a $\frac{1}{\alpha T+\beta T^2}$ behaviour has been reported in the temperature range of 300–800 K.[21] We have previously shown that the same formula can lead to a good fit to experimental data in the laser-induced thermionic emission experiment on carbon nanotube forests for temperatures up to more than 2,000 K.

For each case, we solved equation (1) numerically in order to obtain the temperature as a function of optical intensity, and then evaluated the relative strength of the electron emission term to estimate the conversion efficiency.

[1] C. A. Wolden, J. Kurtin, J. B. Baxter, I. Repins, S. E. Shaheen, J. T. Torvik, A. A. Rockett, V. M. Fthenakis, and E. S. Aydil, J. Vac. Sci. Technol. A, **29**, 030801 (2011).
[2] R. E. Nelson, Semicond. Sci. Technol., **18**, S141 (2003).
[3] W. Schlichter, Annalen der Physik, **352**, 573 (1915), ISSN 1521-3889.
[4] V. C. Wilson, J. Appl. Phys., **30**, 475 (1959).
[5] A. Shakouri, in *24th International Conference on Thermoelectrics* (2005) pp. 507–512, ISSN 1094-2734.
[6] P. Brosens, B. Gunther, S. Merra, and P. G. Pantazelos, *Solar Energy Thermionic (SET) program Final report, task 1*, Tech. Rep. 19680021935 (NASA, 1968).
[7] S. F. Adams, AIP Conf. Proc., **813**, 590 (2006).
[8] P. Yaghoobi, M. V. Moghaddam, and A. Nojeh, Solid State Commun., **151**, 1105 (2011).
[9] Natural Resources Canada, "Natural resources canada - carte pv maps vancouver," (2011), http://pv.nrcan.gc.ca/index.php?n=2170&m=u&lang=e.
[10] J. M. Houston, J. Appl. Phys., **30**, 481 (1959).
[11] J.-H. Lee, I. Bargatin, N. A. Melosh, and R. T. Howe, Appl. Phys. Lett., **100**, 173904 (2012).
[12] M. A. Green, K. Emery, Y. Hishikawa, W. Warta, and E. D. Dunlop, Prog. Photovolt. Res. Appl., **20**, 12 (2012).
[13] J. Che, T. Çağin, and W. A. Goddard, Nanotechnology, **11**, 65 (2000).
[14] R. D. Allen, J. Louis, F. Glasier, and P. L. Jordan, J. Appl. Phys., **31**, 1382 (1960).
[15] P. Yaghoobi, *Laser-Induced Electron Emission form Arrays of Carbon Nanotubes*, Ph.D. thesis, University of British Columbia (2012).
[16] Z.-P. Yang, L. Ci, J. A. Bur, S.-Y. Lin, and P. M. Ajayan, Nano Lett., **8**, 446 (2008).
[17] K. Mizuno, J. Ishii, H. Kishida, Y. Hayamizu, S. Yasuda, D. N. Futaba, M. Yumura, and K. Hata, Proc. Nat. Acad. Sci., **106**, 6044 (2009).
[18] J. W. Schwede, I. Bargatin, D. C. Riley, B. E. Hardin, S. J. Rosenthal, Y. Sun, F. Schmitt, P. Pianetta, R. T. Howe, Z.-X. Shen, and N. A. Melosh, Nat. Mater., **9**, 762 (2010).
[19] A. Hart, L. vanLaake, and A. Slocum, Small, **3**, 772 (2007).
[20] N. W. Ashcroft and N. D. Mermin, *Solid State Physics* (Thomson Learning, 1976).
[21] E. Pop, D. Mann, Q. Wang, K. Goodson, and H. Dai, Nano Lett., **6**, 96 (2005).